Investigation of Iron Oxide Nanocolloidal Suspension Diffusion Using a Direct Imaging Method

Ashley Rice[1] and Ana Oprisan[1*]

[1]*College of Charleston Department of Physics and Astronomy, Charleston, SC*

We performed a set of experiments using a direct imaging method to investigate the diffusion process of iron oxide, Fe_2O_3, nanoparticles. We studied concentration fluctuations that move against the concentration gradient and induce disturbances in the interface between the iron oxide suspension and water in the sample cell. Using this imaging method in combination with the differential dynamic algorithm for image processing, we are able to extract information about the power, size, and lifetime of the fluctuations. We performed this experiment both in the presence and in the absence of a 4.2 mT magnetic field. We find that the power and size of the fluctuations diminish in the presence of a magnetic field, as indicated by the change in slope of the structure factor from approximately -4 to -3, for $q < q_c$. Furthermore, we find that after the removal of the magnetic field, their power and size are still damped beneath those we observed during free diffusion, indicating that the nanoparticles are at least still slightly magnetized. From the lifetime of the fluctuations, we determined the diffusion coefficients of the nanosuspension in each environment.

Introduction

Magnetic nanoparticles have been studied for decades, originally developed into a nanofluid by NASA to aid in the movement of a fluid in zero-gravity conditions.[1] However, in recent years, attention has been turned to these particles and their applications in medicine, including but not limited to MRI contrasting, magnetic cell separation, hyperthermia tumor treatment, biosensors, and drug targeting. Specifically, iron oxide nanoparticles (IONPs) are being highly considered for these areas due to their stability, biocompatibility and non-toxicity, and environmentally safe.[2,3] Due to their large surface-to-volume ration, these nanoparticles are often coated with a polymer to increase their biocompatibility and dispersibility, and extending their applications into the delivery of nucleic acids.[3] These nanoparticles can be readily and inexpensively synthesized in a laboratory setting, adding to their ease of use qualities to be considered for their applications.[2]

To expand upon an application, consider their use in drug targeting. As it stands currently, many drugs are injected. Due to the diffusion of this drug, only a small amount of it will reach its target (a tumor, a pain site, an internal wound, etc). The rest of the drug diffuses away and may cause detrimental effects to surrounding tissues and organs. Using IONPs as a drug carrier, the drug could be encapsulated by these nanoparticles and directed towards a specific target using an external magnetic field, and subsequently released upon arrival at its destination.[2,3] When these nanoparticles are suspended in a colloid, it is possible to control the release of the drug or nucleic acid by manipulating the colloid through the effects of the magnetic field.[3]

It has been observed that nanoparticles on the order of 10-100 nm are of the ideal size for biomedical applications. This is due to the fact that they must be small enough to fit through capillaries, but yet large enough to not be filtered out by the renal system. IONPs of this size are not only useful for cancer drug delivery, but also in drugs that need to reach the brain. The brain is surrounded by a protective blood-brain barrier that functions as a way to keep toxins away from the brain, but often this hinders vital medication from reaching its target. However, IONPs of this size acting as drug carriers provide a safe way of transporting this medicine across the barrier.[2]

In this project investigated the diffusion process of a nanosuspension of iron oxide during the presence and in the absence of a magnetic field. The overarching goal of this project was to determine the diffusion and viscosity coefficients of the Fe_2O_3 nanoparticles. If these nanoparticles are to be used as drug carriers, we must consider the fact that the target area does not have to be near the injection site-in which case we must know information about how long it will take the nanoparticle-coated drug to reach the target, and the effect on the fluid properties as it travels.

Background

Diffusion is a fundamental process in many biological systems, and is the driving force behind biological processes such as gas exchange in the lungs and nerve communication.[4] Defined as the transfer of mass from an area of high concentration to low concentration[4], we investigated the evolution of non-equilibrium concentration fluctuations during this process.

This project was performed using Fe_2O_3 nanoparticles suspended in water, thus creating a suspension called a *nanocolloid*. These nanoparticles are on the size order of 1-10 nm; Therefore, they are small enough to exhibit superparamagnetic properties. Superparagmanetism refers to their magnetic property that in the presence of a magnetic field, these particles become magnetized. Once the magnetic field is removed, however, the particles do not retain their magnetization. This is critical to applications in which these nanoparticles will be travelling through veins or arteries. Their magnetic relaxation upon the removal of the magnetic field prevents them from grouping together and creating a blockage in these areas. Aside from this, it has been observed that the presence of a magnetic field causes the nanoparticles to concentrate in the tissues of a tumor. Another study showed that with the ability to concentrate a drug using a magnetic field, we may be able to cut the dosage by 80%. Once the drug reaches its target, an enzyme or simple physiological changes aid in its release. Many factors contribute to the effectiveness of IONPs as a transport mechanism, such as the depth of the target, blood circulation, as well as the strength and geometry of the applied field. A major area still being explored is how to direct a drug at a target that is not near the surface. The strength of the magnetic field (and thus its overall effects on the IONP carriers) drastically decreases with distance from the source. Proposed solutions include implanting magnets at the target itself to increase the effect of the magnetization.[3]

These nanoparticles are anisotropic in the direction of the applied magnetic field.[3] In order for these particles to become demagnetized, there is a thermal energy barrier to overcome. However, at these sizes room temperature is enough to overcome the energy barrier.[5]

In this paper we investigate results related to the following experiments:

1. Free Diffusion (No magnetic field)
2. Diffusion with a vertical magnetic field
3. Diffusion after the removal of the vertical magnetic field

To contain our nanosuspension, we used a cylindrical Hellma cell, with 2 cm diameter and 2 cm height. Initially, the cell was filled with purified, degassed water. We injected the nanosuspension into the bottom half of the cell, and then drained off the excess water. Initially there was a sharp interface between the nanosuspension in the bottom half of the cell and the water in the top half.

Over time, the interface between the nanocolloid and water will dissipate away as the diffusion progresses and the diffusion process ends when the entire sample cell has a uniform concentration of nanoparticles. The diffusion process begins at this interface, with small pockets of fluids called *concentration fluctuations* that move from the area of high concentration of nanoparticles in the bottom of the cell to the area of low concentration in the top of the cell.[6,7,8,9] During free diffusion, the gradients of concentration and density are competing forces that act on these concentration fluctuations. The downward gravitational force is acting in an effort to return the fluctuation back to its original environment, while the upward concentration gradient is driving the diffusive process in an effort to create a more stable uniform concentration in the cell.[10]

At wavenumbers smaller than a critical wavenumber, gravity quenches these fluctuations. Fluctuations of this range are large enough for the gravitational force to be the dominant force acting on the fluctuations. At concentration fluctuations with wavenumbers larger than the critical wavenumber, the fluctuations are of a small enough mass that gravity does not have a substantial effect on them. At these large wavenumbers, these fluctuations have a long enough lifetime so that diffusion will be the primary mode acting upon them.[6,7,8,9,10]

The primary method of investigation relied on a light scattering technique. It is known that the angles of light scattered depend heavily on the shape of the nanoparticles. While the particles used in this project are strictly spherical, nonspherical nanoparticles have different optical properties that allow them to be used in biomedical diagnositics, circuits in nanodevices, and the load of metal required for metal-polymer fillers[11,12]. Concerning spherical particles of iron oxide, Brojabasi and Phillip found that the optical pattern created by light scattering around the particles is dependent on the strength of the magnetic field interacting with the system.[13] It was found that the backscattered speckle pattern increased with the strength of the magnetic field, and the reversibility of this effect may exhibit potential in the use of these nanofluids for photonic devices.[13]

Through a series of image processing and data analysis techniques known as the *Differential Dynamic Algorithm (DDA)*, we were able to extract information about the physical properties of these fluctuations such as their power spectra, size, and correlation time.[6,7,8,9,14] We investigate the effects of a magnetic field on these properties of the non-equilibrium fluctuations.

Methods

Experimental Design and Direct Imaging

The imaging method used in this project is direct imaging. This technique is valuable as it provides an image of the real space inside the sample cell and thus information about the structure of the interface, as well as the progression of the diffusion process.[14] We use a SONY-XCL-X700 CL CCD camera of resolution 1024 x 768 pixels, with a pixel resolution of 4.65 μm. As we see in Figure 1, the sample cell is mounted to a lens holder on a vertical optical table. For the experiments with a magnetic field, the sample cell is located at the center of a pair of Helmholtz coils that are also mounted to the vertical optical table. We use a light source of wavelength 670 nm that travels from the superluminescent diode to the optical bench via a fiber optic cable. Beneath the sample cell is an achromatic lens that collimates the light so that the sample cell can be illuminated uniformly. The light passes through the cell and is collected by the objective on the CCD camera to produce a real image of the interior of the cell. A close-up image of the sample cell is also presented, with a clear distinction between the iron colloid at the bottom, indicated by its yellow color, and the pure water at the top. The diffusion process is recorded into a movie at a rate of 1 frame per second, and is imported into an in-house MATLAB program. We recorded an entire free diffusion process continuously for 10-12 hours. For experiments involving a magnetic field, we imposed the field for an hour and then removed it for two hours. We repeated this process for several hours and the recorded data then analyzed.

While this paper focuses solely on direct imaging, note that we also performed similar experiments using a shadowgraphy imaging method.[6] Unlike direct imaging, the shadowgraph optical method does not produce a real image of the interior of the sample cell. Rather the images reflect a mapping of the indices of refraction. Direct imaging allows for the determination of the diffusion coefficient, while with shadowgraphy we are able to determine both the diffusion and viscosity coefficients. This is due to the fact that direct imaging is particularly useful for accessing the larger wavenumbers, while shadowgraphy allows access to both small wavenumber fluctuations, which are integral in determining the viscosity coefficient, just as well as it allows the same access to large wavenumbers for the determination of the diffusion coefficient.

Image Processing Methods

The method used to analyze the movie of the diffusion process is a series of steps referred to as the Differential Dynamic Algorithm. This algorithm is listed below as follows:

1. Frame extraction

Frame extraction refers to dividing the movie into individual frames, rather than a continuous progression. These frames were gray level Images. The images were represented as two-dimensional arrays of numbers, with each unit correlating to the intensity of a pixel. The

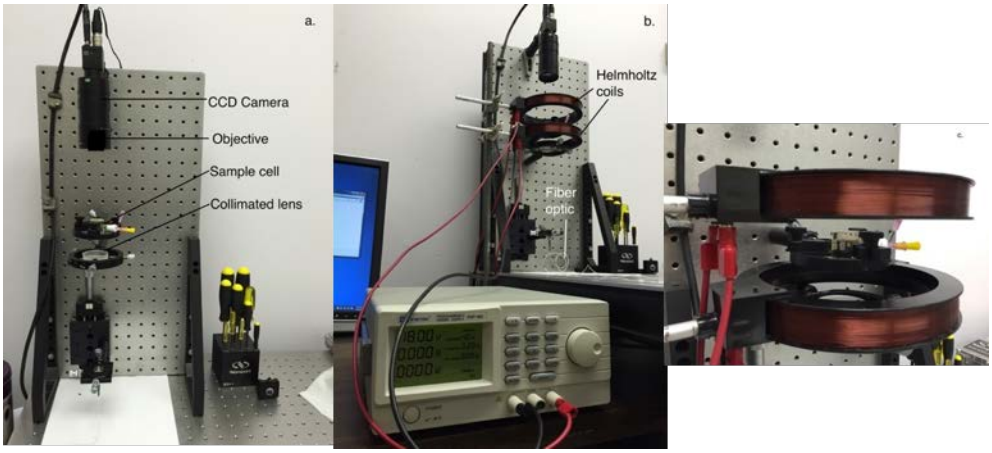

Figure 1. Direct imaging experimental setup

images are first cropped into a 512 x 512-pixel square array, and the pixel in the top left corner will be identified by the position n = 1, the next n = 2, and so on.

2. Normalization of frames

The purpose of normalization of each frame is to decrease the effects of variability of the light source. The normalization process is defined as

$$i(x,t,) = I(x,t)/\overline{I(x,t)}, \qquad (1)$$

and is the process by which every pixel value in the image, $I(x,t)$, is reassigned to a new value. This new value, $i(x,t,)$, is the previous pixel value, $I(x,t)$, divided by the average value of the pixels, $\overline{I(x,t)}$, from the entire image.

3. Fluctuation Image

After all the frames are normalized, we created a new set of images called "fluctuation images." These images are the resultant image after the subtraction of two normalized frames separated by a specific time delay, Δt. We find that for delay times much shorter than 100 s the frames are too correlated and the signal is subsequently subtracted out. Conversely, for delay times much longer than that, the frames were not correlated at all and the fluctuation image consisted of only noise.[6] Mathematically, this operation is represented as

$$\partial i(x,t,\Delta t) = i(x,t+\Delta t) - i(x,t). \qquad (2)$$

4. Two-Dimensional Fourier Transform

On each fluctuation image, $\partial i(x,t,\Delta t)$, we perform a 2D Fourier Transform to convert the image from the spatial domain into Fourier space for analysis. This new image is represented as

$$\partial i(q,t,\Delta t) = FFT2[\partial i(x,t,\Delta t)]. \qquad (3)$$

Note that this new image is not a function of x, the position variable of the spatial domain, but rather a new variable, q, called the wavenumber. In the array of pixels that composes the image, $\Delta\Delta x$ refers to the pixel resolution, or the width of the pixel. Here, Δx = 4.65 microns. We define the wavelength of a fluctuation as

$$\lambda = n\Delta x, \qquad (4)$$

with q following as

$$q = \frac{2\pi}{\lambda}. \qquad (5)$$

5. *Two-Dimensional Power Spectrum.*

The two-dimensional power spectrum is defined as

$$|\partial i(q,t,\Delta t)|^2_{\mathrm{t}} \qquad (6)$$

which we observe in Figure 2.

Averaging outwards away from the center and we obtained power as a function of wavenumber, q. In Figure 2 we see a sample fluctuation image and its power spectrum.

6. *Radial Average Power Spectrum.*
We begin at the center of the ring structure shown in Fig. 2b and average outwards to obtain on the *y*-axis power as a function of radius from the center, and on the *x*-axis we have wavenumber, q. See Figs. 4 and 5. The radial average power spectrum provides information about the evolution of power and its dependence on the wavenumber. The radial average power spectrum is given by

$$c_m(q,t,\Delta t) = Avg(|\partial i(q,t,\Delta t)|^2) \qquad (7)$$

7. *Structure Function.*
To obtain the structure function, we transpose the radial average power spectrum matrix. The structure function, given by

$$C_m(q,t,\Delta t) = Avg[c_m(q,t,\Delta t)]_q \qquad (8)$$

provides information about the temporal evolution of the power, thus a plot of the structure function describes how average of the power changes with time, at constant wavenumbers. The structure function is then fit to

$$C_m(q,t,\Delta t) = 2[S(q,t)T(q) \times \left(1 - e^{-\Delta t/\tau(q,t)}\right) B(q,t)] \qquad (9)$$

and from this fitting we are able to extract the structure factor, $S(q,t)T(q)$, which provides information about how large the concentration fluctuations are, and the correlation time, $\tau(q,t)$, which provides information about the lifetime of the fluctuations. Through a further fitting process to

$$\tau(q,t) = \frac{1}{Dq^2\left(1+\left(q_c/q\right)^4\right)} \qquad (10)$$

we were able to extract the diffusion coefficient, D. In this relation, q_c refers to the critical wavenumber.

Results and Discussion

Fluctuation Image and Two-Dimensional Power Spectrum

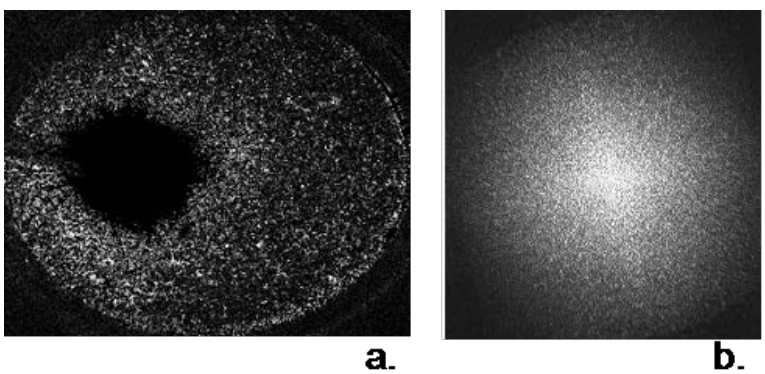

Figure 2. a.) Fluctuation image determined by subtracting two normalized frames at a time delay of Δt = 100 s. The large dark area is the subtracted region where the light source is fed into the system underneath the sample cell. This figure gives a top down view into the sample cell. b.) Corresponding power spectrum after performing a 2D FFT on the fluctuation image.

For comparison, in Figure 3 we see an example of a fluctuation image obtained using the shadowgraphy method. The dark areas represent regions in which the light does not easily come through due to large concentration of nanoparticles in these regions. The bright areas indicated regions with a relatively small refractive index due to the region having a low concentration of nanoparticles.

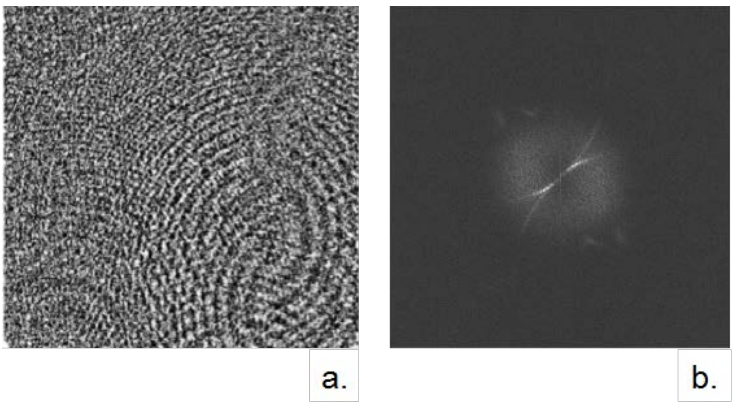

Figure 3. a.) Fluctuation image obtained using the shadowgraphy optical method for free diffusion. b.) The corresponding power spectrum.

Radial Average Power Spectrum

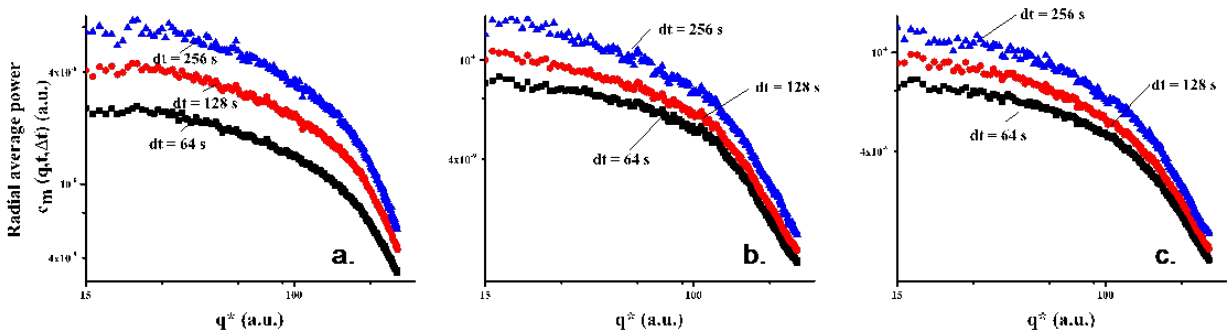

Figure 4. a.) Free diffusion. b.) During exposure to a vertical magnetic field. c.) After removal of magnetic field. We infer that the magnetic field is quenching the concentration fluctuations due to a decrease in the amplitude of the power spectrum that occurs in the case with the imposed magnetic field, and even the case after the vertical field is removed, which is indicative that these particles are still magnetized after the removal of the field.

Note that the largest delay times yield the highest amplitudes in the radial average power spectrum. Subtracting two images that differ by a larger amount of time produces a resultant fluctuation image that has a stronger signal with more power, so this is what we expect to see here.

For comparison we have included a power spectrum that makes a direct comparison between the free diffusion case with the magnetic field cases. Note the damping of the amplitude in Figure 5.

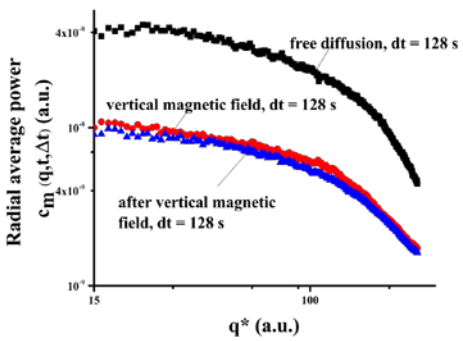

Figure 5. Power spectrum comparison at a delay time of 128 s. Nanoparticles that have been exposed to a magnetic field, even if not currently exposed to a magnetic field, still exhibit a smaller amplitude of the power spectrum than that of free diffusion.

Structure Function

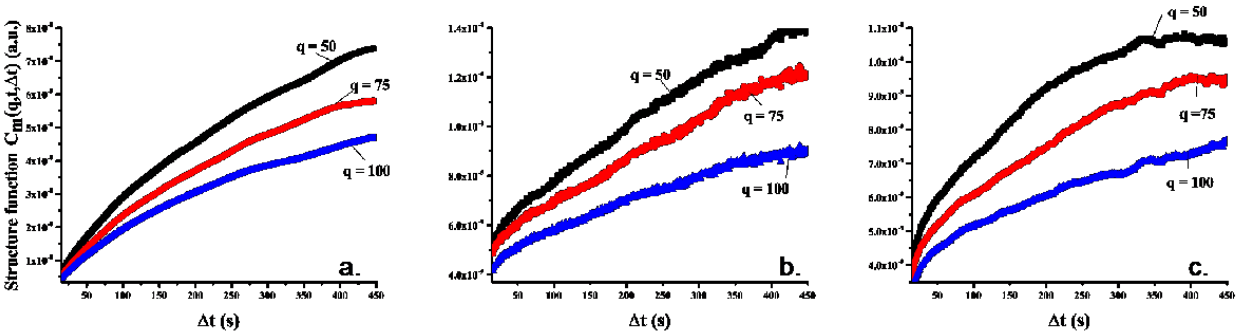

Figure 6. a.) Free diffusion. b.) During exposure to a magnetic field. c.) After removal of a magnetic field. Like in the radial average power spectrum, we again observe the effects of quenching from the magnetic field given by the decreased amplitude of the structure function in these cases.

Recall that the structure function provides information about the temporal evolution of the power spectrum. Thus when we plot the structure function against time, we do expect an upward slope as seen in Figure 6 because the signal strength will increase with an increase in delay time between frames. Also note that the smallest wavenumber has a much larger amplitude than the other wavenumbers. This is due to the fact that the wavenumber and size of the fluctuation are inversely proportional, so the smallest wavenumber actually corresponds to the largest concentration fluctuation. Therefore, we expect that the smallest wavenumber would have the largest structure function. Were we to take a cross-sectional slice of the structure function, we would observe exactly how the wavenumber is evolving as well.

Structure Factor

From the fitting of the structure function using Eq. (9), we were able to obtain the structure factor, which provides information about the size of the fluctuations, as well as their correlation time, $\tau(q,t)$.

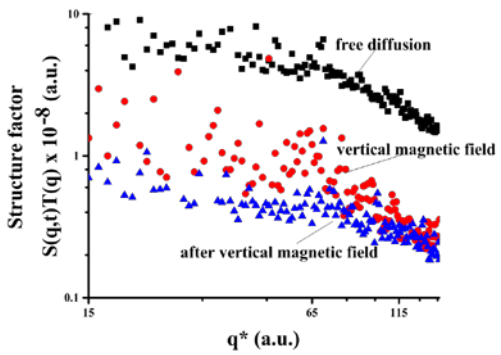

Figure 7. Side-by-side comparison between free diffusion and the magnetic field cases. We observe that the fluctuations are of the largest size when they are not exposed to a magnetic field, indicative that the magnetization is quenching the amplitude of the fluctuations.

Note that the structure factor, $S(q,t)T(q)$ is actually a product of the true structure factor, $S(q,t)$, and the transfer function of the optical system, $T(q)$. For the Schlieren method, however, $T(q) = 1$, and therefore $S(q,t)$ coincides with $S(q,t)T(q)$. We observe a relatively flat slope at first for $q < q_c$, and then a steep drop-off of a slope approximately -4 for $q > q_c$, corresponding to a power law slope of q^{-4}. This is seen in the free diffusion case. In the magnetic field experiments, this slope is decreased to q^{-3}. The sharp change in slope occurs at the critical wavenumber, q_c, which is the wavenumber at which the diffusive process then becomes the dominant force acting on the fluctuations.

Correlation time

The correlation time provides information about the lifetime of the concentration fluctuations and was extracted using Eq. (9). We were able to observe the gravitational and diffusive effects in plots of the correlation time.

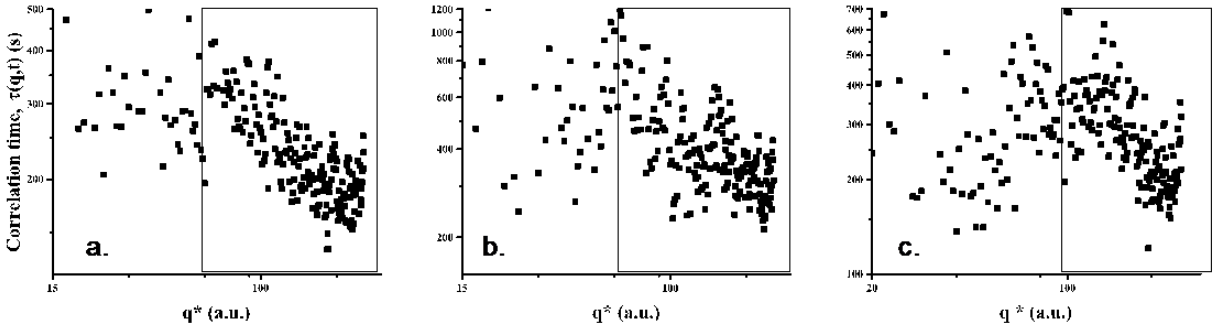

Figure 8. a.) Free diffusion. b.) During exposure of a magnetic field. c.) After removal of magnetic field. The un-shaded region corresponds to the gravitational effect region and the shaded region corresponds to the region that the diffusive process is the dominant force

We observed that between the gravitational and diffusive regimes there is a change in concavity. This is at the critical wavenumber, q_c, which tells us about the size of the fluctuations at which it is small enough such that it is not effected as much by gravity, and therefore does not get quenched out immediately. At this wavenumber, the fluctuation has a long enough lifetime such that diffusion is able to act on it.

From the fitting of the correlation time using Eq. (10) we were able to determine the diffusion coefficient for the nanocolloid. Note, however, that these values were not determined using the direct imaging method, but rather the shadowgraphy optical method. We found that $D = (8.3 \pm 3.6) \times 10^{-10}$ cm^2/s for free diffusion, $D = (3.2 \pm 1.4) \times 10^{-10}$ cm^2/s during the exposure to a magnetic field, and $D = (4.9 \pm 1.8) \times 10^{-10}$ cm^2/s after the magnetic field is removed. The fitting process that was used in the shadowgraphy method to extract these results is the exact process that would be used in the direct imaging method.

Conclusions

Using a direct imaging method, we investigated the diffusive process of Fe_2O_3 nanoparticles. We performed three experiments. The first experiment was in a free diffusion environment, i.e. without influence of a magnetic field. The second experiment was performed under the influence of a 4.2 mT magnetic field. The third experiment was conducted after the magnetic field was removed. We find that the structure factor maintains a power law q^{-4} for diffusion in the absence of a magnetic field. This is indicative of large concentration fluctuations occurring at the interface. In the presence of the magnetic field, we find that the structure factor slope decreases to a power law of q^{-3}. In addition, we also find that the slope of the diffusion regime observed in the correlation time follows a q^{-2}, and the gravitational regime follows a q^2 power law, which is also indicative of large concentration fluctuations. After the magnetic field is removed and the system is once again in a free diffusion environment, we find that the size of the fluctuation is still damped beneath that of the fluctuations observed before the addition of a magnetic field. This is evidenced by the fact that the slope of the structure has not recovered to its initial q^{-4}. From the diffusion coefficient D, we do see evidence that the magnetization relaxes over time, but it is not instantaneous.

We repeated this experiment using a shadowgraphy method and the same Differential Dynamic Algorithm. Using the shadowgraph optical method, it was found that the diffusion coefficient decreased in the presence of a magnetic field, likely due to the formation of nanorods[6]. As the magnetic field is applied, the nanoparticles align in the direction of the magnetic field, and subsequently aggregate together into chainlike structures, consisting of 100-9000 particles[6]. This is thought to be the cause of backscattering of the incident light and decrease the overall light intensity that is detected.[13] More investigation is required to understand the mechanism behind the quenching of the concentration fluctuations, however.[6]

Acknowledgements

We are grateful to Drs. Fabrizio Croccolo and Cédric Giraudet for discussion on the experimental design and computational methods. We also thank Dr. Sorinel Oprisan for his assistance on the computational work. This project was funded by a Summer Undergraduate Research with Faculty (SURF) grant awarded to Ashley Rice and Dr. Ana Oprisan. This research was supported by a grant from the Howard Hughes Medical Institute to the College of Charleston as part of their 2012 Undergraduate Science Education Competition.

Notes and References

**Corresponding author E-mail: oprisana@cofc.edu*

1. John Philip and Junaid M. Laskar. 2012. Optical Properties and Applications of Ferrofluids- A Review. Journal of Nanofluids Vol. 1: Pg. 3-20
2. Wei Wu, Zhaohui Wu, Taekyung Yu, Changzhong Jiang, Woo-Sik Kim. 2015. Recent Progress on magnetic iron oxide nanoparticles: synthesis, surface functional structures, and biomedical applications. Science and Technology of Advanced Materials Vol. 16: Pg. 23501-23545.

3. Joan Estelrich, Elvira Escribano, Josep Queralt, Maria Antònia Busquets. 2015. Iron Oxide Nanoparticles for Magnetically-Guided and Magnetically-Responsive Drug Delivery. International Journal of Molecular Sciences Vol. 16: Pg. 8070-8101.
4. David Nguyen. 2017. Sciencing. [cited 05 May 2017]. Available from: http://sciencing.com/importance-diffusion-organisms-20189.html.
5. Manuel Benz. 2012. Superparamagnetism: Theory and Applications.
6. Ana Oprisan, Ashley Rice, Sorinel Oprisan, Cédric Giraudet, Fabrizio Croccolo. 2017. Non-equilibrium concentration fluctuations in superparamagnetic nanocolloids. European Physical Journal E Vol. 40: Pg. 14-26.
7. Fabrizio Croccolo. 2015. Dynamics of non equilibrium fluctuations in free diffusion. PhD thesis. Università degli Studi di Milano. Milano, Italy.
8. Ana Oprisan, Alexis Leilani Payne. 2013. Dynamic shadowgraph experiments and image processing techniques for investigating non-equilibrium fluctuations during free diffusion in nanocolloids. Optics Communications Vol. 290: Pg. 100-106.
9. Ana Oprisan, Sorinel Oprisan, Alem Teklu. 2010. Experimental study of nonequilibrium fluctuations during free diffusion in nanocolloids using microscopic techniques. Applied Optics Vol. 49, No. 2: Pg. 86-98.
10. Fabrizio Croccolo, Doriano Brogioli, Alberto Vailati, Marzio Giglio, David S. Cannell. 2006. Effect of gravity on the dynamics of nonequilibrium fluctuations in a free diffusion experiment. Annals New York Academy of Sciences Vol. 1077: Pg. 365-379.
11. A.V. Alekseeva, V.A. Bogatyrev, B.N. Khlebtsov, A.G. Mel'nikov, L.A. Dykman, and N.G. Khlebtsov. 2006. Gold Nanorods: Synthesis and Optical Properties. Colloid Journal Vol. 68, No. 6: Pg. 725-744.
12. Krasimir Vasilev, Tao Zhu, Michael Wilms, Graeme Gillies, Ingo Lieberwirth, Silvia Mittler, Wolfgang Knoll, and Maximilian Kreiter. 2005. Langmuir Vol. 21: Pg. 12399-12403.
13. Surajit Brojabasi and John Philip. 2013. Magnetic field dependent backscattering of light in water based ferrofluid containing polymer covered Fe_3O_4 nanoparticles. Journal of Applied Physics Vol. 113: Pg. 54902-54908.
14. Ana Oprisan, Sorinel A. Oprisan, John J. Hegseth, Yves Garrabos, Carole Lecoutre, Daniel Beysens. 2015. Direct imaging of long-range concentration fluctuations in a ternary mixture*. European Physical Journal E Vol. 38: Pg. 17-28.